

# PHYSICAL REVIEW C

## NUCLEAR PHYSICS

THIRD SERIES, VOLUME 42, NUMBER 5

NOVEMBER 1990

### RAPID COMMUNICATIONS

*The Rapid Communications section is intended for the accelerated publication of important new results. Manuscripts submitted to this section are given priority in handling in the editorial office and in production. A Rapid Communication in Physical Review C may be no longer than five printed pages and must be accompanied by an abstract. Page proofs are sent to authors.*

#### Spins in superdeformed bands in the mass 190 region

J. E. Draper,\* F. S. Stephens, M. A. Deleplanque, W. Korten, R. M. Diamond, W. H. Kelly,<sup>†</sup> F. Azaiez,<sup>‡</sup>  
A. O. Macchiavelli, C. W. Beausang,<sup>§</sup> and E. C. Rubel\*

*Nuclear Science Division, Lawrence Berkeley Laboratory, Berkeley, California 94720*

J. A. Becker, N. Roy, E. A. Henry, M. J. Brinkman,\*\* A. Kuhnert, and S. W. Yates<sup>††</sup>

*Lawrence Livermore National Laboratory, Livermore, California 94550*

(Received 18 May 1990)

A method to determine spins,  $I$ , associated with transitions in superdeformed rotational bands in the mass 190 region is described and analyzed for conditions of validity. It contributed significantly to two recent articles proposing the relevance of pseudospin to some of these bands. An expansion of  $dI/d\omega$  in even powers of the rotational frequency,  $\omega$ , is fitted, and its extrapolation down to  $\omega=0$  is integrated to obtain  $I$ . Typical errors for data with smaller backgrounds are  $0.05\hbar-0.1\hbar$ . A related method employing directly an expansion of the spins in odd powers of  $\omega$  is briefly compared to this method. The  $dI/d\omega$  method has advantages for the crucial task of assessing the fit in the extrapolation region.

Superdeformed (SD) rotational bands in the mass 190 region have received considerable attention recently.<sup>1-5</sup> However, in no case have the spins in a SD band been determined by direct experiment. Two empirical methods<sup>6</sup> have been developed for determining these spins, in favorable cases, from the energies of the  $\gamma$ -ray transitions within the SD bands. More recently many SD bands in different nuclei in the mass 190 region (hereafter denoted SD190) have been found to bear a remarkably strong resemblance to each other, having spin alignments, relative to a reference SD band, of 0, 1, or 2 within a few hundredths. (We use units of  $\hbar=1$ .) This observation has been linked<sup>7,8</sup> to ideas of pseudospin, pseudo-oscillator, and perhaps pseudo-SU3. Our means of obtaining the spins in the bands have contributed substantially to these important comparisons, and it is important to explore and test the methods for accuracy and limitations. In this paper we will examine mainly the method based on a dynamical moment of inertia ( $J^{(2)}$ ) expansion. Another paper<sup>6</sup> explores the other method, but we will discuss it here briefly also.

Typically, superdeformed bands have about a dozen nearly evenly (closely) spaced  $\gamma$ -ray transition energies,

$E_\gamma$ . Angular correlation data indicate that the transitions are stretched quadrupole ( $I_i - I_f = 2$ , where  $I_i$  and  $I_f$  are the initial and final spins of the transition).

Our approach centers on Eqs. (1) and (2), whose derivation is somewhat related to that of the Harris expansion,<sup>9</sup> derived for results from the cranking model. Harris expands the energy in a power series in the square of the cranking frequency, in order that the energy be independent of the sign of the direction of cranking (sign of the cranking frequency). The resulting expectation value of the cranking-axis component of the spin is then an odd-power series in the cranking frequency, the two changing sign together, as expected. Harris then uses that same power series to approximate  $[I(I+1)]^{1/2}$ , whose dependence on the *sign* of the cranking frequency is no longer physically reasonable. We take a somewhat different, model-independent tack. Our derivation of Eqs. (1) and (2) only needs (a) the level energy  $E$  to be well approximated by an even-power series in  $\omega$ , where  $\omega = dE/dI = E_\gamma/2$ , and (b) the mathematical relation  $dE/d\omega = (dE/dI)(dI/d\omega)$ . This functional dependence on  $\omega^2$  is similarly reasonable, considering the familiar semiclassical identification of  $\omega$  with rotational frequency. Neverthe-

less, our assumption (a) is always tested by a plot of  $4/\Delta E_\gamma = dI/d\omega = J^{(2)}$  against  $(E_\gamma/2)^2$ , as shown in the figures. (Each point is plotted at the average of its two  $E_\gamma$ 's). For SD190 such a data plot is nearly linear, so a power series in  $\omega^2$  is used with, at most, a small  $\omega^4$  term and negligible higher-order terms. The fits are good. The effect of the replacement of differentials by finite differences ( $dE \approx E_\gamma$ ,  $d\omega \approx \Delta E_\gamma/2$ ) will be tested by fits to Eq. (3).

Regarding Eqs. (1) and (2) more generally, for a dummy variable  $Z$  representing  $I$ ,  $I_x$ ,  $[I(I+1)]^{1/2}$ , or  $I + \frac{1}{2}$ , if another dummy variable  $W$  is defined as  $dE/dZ$ , and the experimental  $dZ/dW$  can be accurately fit by a function of  $W$  which can be convincingly extrapolated to  $W=W_0$ , and  $Z(W_0)$  is known, then  $dZ/dW$  can be integrated to obtain  $Z$  at the bottom of the band. We have chosen, and this paper uses,  $Z=I$ , having the simplest  $\Delta Z$ , namely 2, and the simplest relation to spin  $I$ . Most important, this gives good SD190 fits, and enables convincing demonstration that the spins from our fits are almost always within 0.1 of being an even or odd, as appropriate, integer multiple of  $\frac{1}{2}$ .  $Z=I$  and  $I + \frac{1}{2}$  would give identical spins  $I$ .

Using the assumption (a) and mathematical relation (b), one immediately gets

$$J^{(2)} = 4/\Delta E_\gamma = dI/d\omega = A + B\omega^2 + C\omega^4. \quad (1)$$

Integrating this with respect to  $\omega$  gives

$$I_\gamma(\omega) - I_{\gamma 0} = A\omega + (B/3)\omega^3 + (C/5)\omega^5. \quad (2)$$

The coefficients  $A$ ,  $B$ , and  $C$  in Eq. (2) are obtained by least-squares fitting of  $J^{(2)}$  vs  $\omega^2$ . (The units for  $A$ ,  $B$ , and  $C$  will be appropriate to  $\omega$  being in MeV.)

There are many nuclei for which the level energies of a substantial portion of a rotational band can be reasonably described in the form

$$E = [(I-i)(I-i+1) - K^2]/2J^{(0)}, \quad (3)$$

with constants  $i$  and  $K$ , and with  $J^{(0)}$  varying, at most, slowly with  $I$ , so Eq. (3) is suitable for use as a test of the method. In the strong coupling limit of the particle-rotor model, Eq. (3) (with an inconsequential additive constant) applies, where  $i=0$ , and  $K$ =bandhead spin. In the decoupling limit (rotational alignment) of that model, and a single  $j$  shell, Eq. (3) similarly applies where  $i$  is a constant, and under representative conditions there is a cancellation of the  $K$  dependence. On the other hand, setting  $i=0$  gives the numerator the familiar form of  $I_x^2$  of the cranking model. It will be seen that the present methods of spin determination work properly for all versions of Eq. (3) when  $|C|$  is not large, as discussed below.

One needs  $I_{\gamma 0}$  for use in Eq. (2). For cases obeying Eq. (3) and having  $I_i - I_f = 2$ , then  $E_\gamma = [4(I_i - i) - 2]/2J^{(0)}$ . Thus  $\omega=0$  at  $(I_i + I_f)/2 = i - \frac{1}{2}$ , and the left-hand side of Eq. (2) is  $I_\gamma(\omega) - i + \frac{1}{2}$ . Correcting for the  $\frac{1}{2}$ , as we do, the fit yields  $I_\gamma(\omega) - i$ , and  $i$  cannot be directly determined. Illustrating, for a  $K = \frac{1}{2}$  band the  $E_\gamma$ 's of a strong-coupled band are given by Eq. (3) if  $i$  is replaced by  $\pm a/2$  (depending on signature), and  $K^2$  is replaced by another constant related to the decoupling parameter (constant)  $a$ . For most of SD190 we believe<sup>2,3</sup> that Eq.

(3) with  $|i| \lesssim 0.1$  is applicable, since most spins are found to be within  $\pm 0.1$  of an integer or half integer, as appropriate. This is explored in Refs. 7 and 8, with interesting results.

In order to test the method, artificial  $E_\gamma$ 's were generated using Eq. (3). The form chosen for  $J^{(0)}$  was

$$J^{(0)} = a + bI^2 + cI^4, \quad (4)$$

with  $a=90$  MeV<sup>-1</sup> (appropriate for SD190) and a variety of coefficients  $b$  and  $c$ . The tests often used  $I_i = 10, 12, \dots$ , or  $\frac{21}{2}, \frac{23}{2}, \dots$ , or  $11, 13, \dots$ , giving an appropriate extrapolation (from  $\omega=0$  to lowest  $\omega$  in the band) region, such as arises from a bandhead with large spin, or from leaving a band before the bandhead, as in SD190. The form of Eq. (4) gives  $J^{(2)}$ 's containing only even powers of  $\omega^2$ , but with small terms beyond  $\omega^4$ , so the least-squares fit using Eq. (1) with no powers beyond  $\omega^4$  will not give an exact fit to these  $J^{(2)}$ 's. The  $E_\gamma$ 's were randomized according to the assumed uncertainty, with little effect on the results.

A representative result using Eqs. (3) and (4) is shown in Fig. 1 and Table I. The six  $J^{(2)}$ 's (5-10) included in the least-squares fit using  $C=0$  (denoted  $AB$  fit) are circled. The assigned uncertainties in  $E_\gamma$  were 0.1 keV, producing  $J^{(2)}$  errors almost too small to be visible. Figure 1(b) shows the differences ( $x$ 's) between the spins deduced from the fit (solid line) in Fig. 1(a) and the correct spins. The input parameters were  $i=0=K$  and  $J^{(0)} = 90[1 + 0.1(I/40)^2 - 0.02(I/40)^4]$  MeV<sup>-1</sup>, with the six fitted transitions having  $I_i = 10, 12, \dots, 20$ . This  $J^{(2)}$

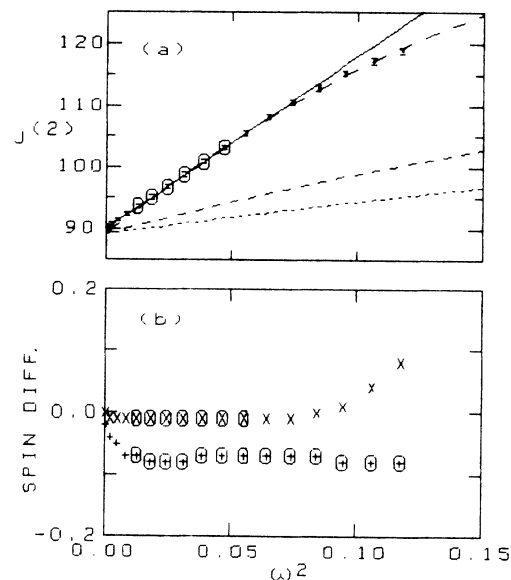


FIG. 1. (a) Moment of inertia  $J^{(2)}$  vs  $\omega^2$  for artificial  $E_\gamma$ 's from Eqs. (3) and (4) with parameters given in text. Circled points were used in  $AB$  fit to Eq. (1), solid line, and Table I. The long-dashed curve is  $ABC$  fit to  $J^{(2)}$ 's 5-17. For comparison, the short-dashed curve is  $J^{(1)}=I/\omega$ , and dotted curve is  $J^{(0)}$ , Eq. (3). (b) Differences between spins from Eq. (2) and correct spins, using  $A$ ,  $B$ , and  $C$  from fits in (a). The  $x$ 's are  $AB$  fit;  $+$ 's are  $ABC$  fit; circled points [one more in (b) than in (a)] were used in fits in (a).

TABLE I. *AB* spin fits,  $I_{\gamma 1}$ , by the  $J^{(2)}$  method, Eqs. (1), (2), or by the *I* fit method, Eq. (5). Num identifies the fitted  $J^{(2)}$ 's or transitions, respectively.

	Artificial		$^{192}\text{Hg}$		$^{194}\text{Hg}^*$		$^{233}\text{U}$	
	$J^{(2)}$	<i>I</i> fit	$J^{(2)}$	<i>I</i> fit	$J^{(2)}$	<i>I</i> fit	$J^{(2)}$	<i>I</i> fit
Num	5-10	5-11	1-6	1-7	1-5	1-6	4-8	4-9
$E_{\gamma 1}$	208.9		214.6		262.6		223.6	
<i>A</i>	89.8	89.8	88.2	88.2	93.7	93.9	84.3	84.2
$\sigma_A$	0.36	0.22	0.36	0.23	0.68	0.53	1.0	0.7
<i>B</i>	281	281	338	337	243	237	1239	1237
$\sigma_B$	12	8	12	8	19	15	42	30
$I_{\gamma 1}$	8.99	8.99	9.10	9.10	11.98	12.00	9.50	9.49
$\sigma_{I 1}$	0.03	0.02	0.03	0.02	0.08	0.06	0.09	0.07

curve is similar to that of  $^{192}\text{Hg}$ , Fig. 2. The long-dashed curve in Fig. 1(a) is an *ABC* (all three coefficients used) fit to  $J^{(2)}$ 's 5-17 [circled +’s in Fig. 1(b)], giving  $C = -620 \pm 120$  and  $I_{\gamma 1} = 8.93 \pm 0.03$ . In other tests,  $K^2$  was varied from 0 to 36 with essentially no effect on the fitted  $I_{\gamma}$ 's.

The uncertainties  $\sigma_{I 1}$  in the spin, Table I, are purely statistical, and are obtained as follows. The least-squares fitting gives simultaneous equations which are solved by matrix methods. In that process the error matrix (inverse of the square matrix) is found, whose diagonal elements are the variances of *A*, *B*, and *C*, providing  $\sigma_A$ ,  $\sigma_B$ , and  $\sigma_C$ . The large off-diagonal elements show that the errors here are substantially correlated. Uncertainties listed in this paper (apart from the following estimates) are from all these matrix elements.

To elucidate this spin uncertainty, with a geometric argument one can estimate  $\sigma_{I 1}$  for a nearly linear  $J^{(2)}$  vs  $\omega^2$  plot as  $\sigma_J \omega_1 (2R + 1)/4$ , where  $\sigma_J$  is a typical uncertainty in  $J^{(2)}$ ,  $\omega_1$  is the frequency for the first transition in the

fitting span, and *R* is the ratio of  $\omega^2$  at the middle of the span divided by half the difference of the  $\omega^2$ 's at the ends of the span. In Fig. 1 and Table I, e.g.,  $\omega_1 = 0.209$ ,  $R = \frac{0.108}{0.0644}$ , and 0.1 keV uncertainty in transition energies gives  $\sigma_J = 0.30$ . These values give 0.034 as the estimated spin uncertainty, in good agreement with the error matrix result,  $\sigma_{I 1} = 0.03$ , in the bottom row of Table I. For the other three cases in Table I, the estimated spin uncertainties are, respectively, 0.035, 0.064, and 0.097.

An important consideration is the span of points to include in a fit to provide a valid set *A*, *B*, *C* (denoted  $\{ABC\}$ ) in the extrapolation region. Plotting  $J^{(2)}$  against  $\omega^2$  provides the best means of detecting the presence of a band crossing in or near the first half dozen transitions, which could compromise the accuracy of  $\{ABC\}$  in the extrapolation region. If one somehow knew that a single  $\{ABC\}$  applied to the entire range of data and extrapolation, then the best spin would result from fitting all the points, starting from the lowest  $J^{(2)}$ . However, if there is a band crossing commencing in the higher  $\omega$ 's of the data, it is better to use only the first few  $J^{(2)}$ 's, even though the  $\sigma_I$  from the error matrix is larger. A possible criterion is to fit SD  $J^{(2)}$ 's 1 to *N*, where *N* represents the first  $J^{(2)}$  that results in  $\sigma_{I 1} \leq 0.1$ . Since the first observed transition is usually weak, with attendant larger and more uncertain energy errors, it may sometimes be better to omit it. Also it is found that the error matrix from an *AB* fit usually gives a substantially smaller  $\sigma_{I 1}$  than that from an *ABC* fit. This can be true even for a long-span fit with significant curvature where the  $J^{(2)}$  vs  $\omega^2$  plot shows the *ABC* fit to be obviously superior. That is,  $\sigma_{I 1}$  from the error matrix is not the whole story, since a least-squares fit assumes that the *form* of the fitting curve is correct. Consequently, the figures include examples of both short- and long-span fits. On the other hand, if there were a band crossing below the data, too narrow and too low in energy to give any indication in the  $J^{(2)}$  vs  $\omega^2$  plot, the  $\omega$ 's would be more closely spaced there (i.e., increased  $J^{(2)}$ ). Then the method would assign spins too small by exactly the amount of alignment (i.e., missed extra area in  $J^{(2)}$  vs  $\omega$ ) produced by the crossing.

Many other tests with Eq. (4) were made, and the errors in spin were  $< 0.1$  for all cases with fitted  $|C| \leq 1000$ , also satisfied by SD190. Larger values of  $|C|$  [curvature in Fig. 1(a)] beyond 2000 made larger errors in spin, but an error of only 0.12 was found in fitting  $J^{(2)}$ 's

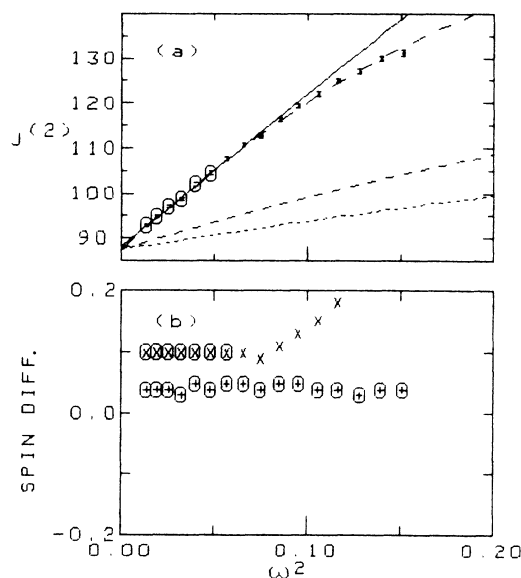


FIG. 2. Like Fig. 1, but for yrast SD band in  $^{192}\text{Hg}$ . (b) Like Fig. 1(b), but x's are an *AB* fit to  $J^{(2)}$ 's 1-6, and +’s are an *ABC* fit to  $J^{(2)}$ 's 1-15. Ordinate is  $I_{\gamma}$  spins minus 9.0, 11.0, . . .

6–12 for  $J^{(0)} = 90[1 + 0.15(I/40)^2]$ , resulting in  $B = 273$ ,  $C = 5294$ . For SD190,  $|C|$  is not large, as seen below. We aimed for  $|C| \lesssim 1000$  because: (i) For typical uncertainties in  $E_\gamma$ , a too-large-span fit is needed to evaluate a large  $|C|$  with sufficient accuracy for good spin determination. (ii) A large  $|C|$  is apt to be accompanied by a need for higher powers of  $\omega^2$  than are present in Eqs. (1) and (2).

For SD190 the conditions are favorable for the application of the present method, viz., spin only  $\sim 10$  at the bottom of the band, and  $J^{(2)}$  vs  $\omega^2$  nearly linear, leaving little possibility for an undetected change of shape for  $J^{(2)}$  below the data. Figure 2 shows the SD band<sup>2</sup> in <sup>192</sup>Hg. Uncertainties in  $E_\gamma$  of 0.1 keV were compatible with the experimental results and the fit. The solid line is the *AB* fit of Table I. The long-dashed curve is an *ABC* fit to  $J^{(2)}$ 's 1–15, giving  $I_{\gamma 1} = 9.04 \pm 0.03$  and  $C = -555 \pm 85$ . (For a fitting span of 1–8, or smaller,  $\sigma_C$  is larger than  $|C|$ , as discussed above.)

This <sup>192</sup>Hg band is especially important to the considerations of pseudospin and pseudo-oscillator<sup>7,8</sup> since it is the reference band. These results show that an *ABC* fit is compatible with integer spin 9, i.e.,  $9.04 \pm 0.03$ . On the other hand, the *AB* fit is physically safer, as discussed above, but Table I gives 9.1, slightly different because the *AB* fit neglects the (small) curvature in  $J^{(2)}$ , Fig. 2.

Figure 3 shows a weak excited SD band<sup>3</sup> in <sup>194</sup>Hg. The  $J^{(2)}$  data are more scattered, probably caused by the weakness of the band, requiring subtraction of a background having peaks much more intense than the SD band. The quoted uncertainties in  $E_\gamma$  were used. The first eleven  $J^{(2)}$ 's are nearly linear, so *AB* fits are shown in Fig. 3; *ABC* fits gave very similar results. The solid line, span 1–5, gives  $I_{\gamma 1} = 11.98 \pm 0.08$ . The long-dashed fit,  $J^{(2)}$  span 1–12, is an example of an unnecessarily large span, and gives  $I_{\gamma 1} = 11.92 \pm 0.05$ .

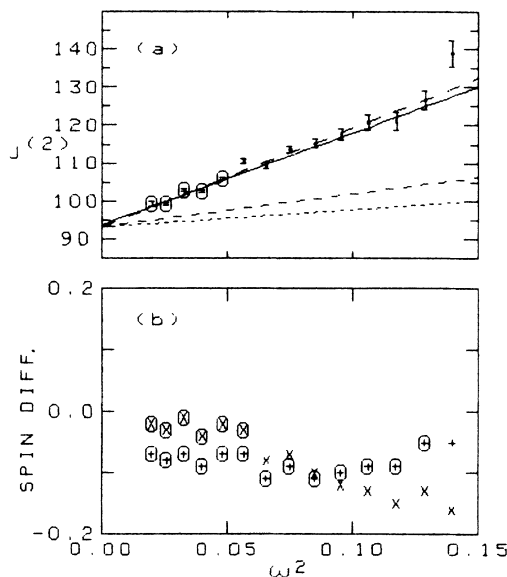


FIG. 3. Like Fig. 1, but for a weak, excited SD band in <sup>194</sup>Hg. Solid curve is *AB* fit to  $J^{(2)}$ 's 1–5; long-dashed curve is *AB* fit to  $J^{(2)}$ 's 1–12. (b)  $I_\gamma$  spins minus 12.0, 14.0, . . . . The x's are for the 1–5 span; +'s are for 1–12 span.

Another illustration of the method would use experimental data for bands having large (but not SD) values of  $J^{(2)}$ , with all spins known, with *ABC* fits adequate, and with  $|C|$  not too large. It is very difficult to find such bands, apart from SD190, so this test was not discussed earlier. Eighteen bands studied by multiple Coulomb excitation in the actinides were analyzed, and only one, a  $K = \frac{5}{2}$  band<sup>10</sup> in <sup>233</sup>U, was found with  $|C| < 1000$  and a smooth curve of  $J^{(2)}$  vs  $\omega^2$ . An *AB* fit to this band, using  $E_\gamma$  errors of 0.15 keV, is shown in Fig. 4 and Table I, yielding the correct spin nicely. Five other bands had a significant hook shape in the  $J^{(2)}$  plot at low spins, one other had a linear  $J^{(2)}$  vs  $\omega^2$  but a sudden jump in the lowest  $J^{(2)}$ , ten others had  $C$ 's ranging from 10000 to 37000, and one other had  $C = 5000$ . Nevertheless, for fourteen bands (some with slow alignment found in the cranking model) when *all* the first five to nine  $J^{(2)}$ 's down to the bandhead were fitted, the corresponding spins of all those six to ten transitions were correct within 0.15, illustrating that Eq. (1) can even follow a slow alignment faithfully—a welcome result. (The significance of “five to nine” is the number of  $J^{(2)}$ 's before a clearly different behavior of  $J^{(2)}$  vs  $\omega^2$  sets in). The other four bands had spin errors of 0.24–0.33, caused by the above jump in  $J^{(2)}$ , or  $C = 37000$ , or a hook shaped  $J^{(2)}$ , or a combination of  $C = 20000$  and erratic behavior of  $J^{(2)}$  vs  $\omega^2$ . For the fourteen bands, above, the difficulty was that the  $J^{(2)}$  vs  $\omega^2$  plot showed too few transitions belonging to the same  $\{ABC\}$  to provide reliable spins while ignoring the first four or more transitions for a simulated extrapolation region. That is, a large-span fit is required to evaluate  $C$  sufficiently accurately when  $|C|$  is large. On the other hand, with large  $|C|$  and a four-transition extrapolation an *AB* fit is obviously unsatisfactory, being linear in the presence of large curvature. Fortunately, the SD190 cases

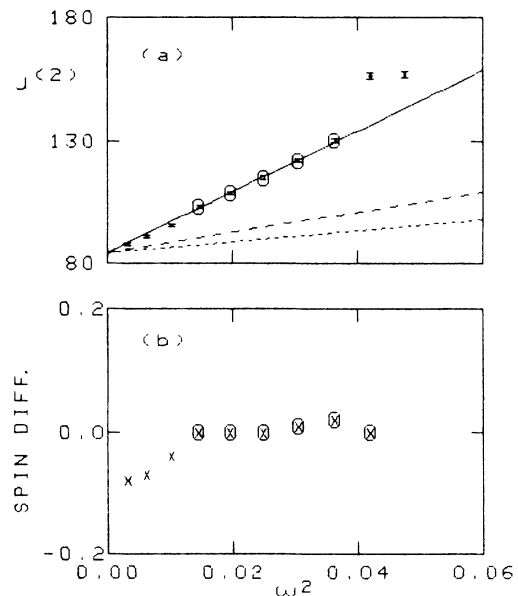


FIG. 4. Like Fig. 1, but for  $K = \frac{5}{2}$  band in <sup>233</sup>U. (a) Solid curve is *AB* fit to  $J^{(2)}$ 's 4–8. (b) Spins minus experimental spins.

do not have these problems.

Another approach<sup>6</sup> to finding spins would be to expand the spins directly in odd powers of  $\omega$ , assuming the form of Eq. (2), while forcing the spins to increase successively by 2. Mathematically, this approach is very similar to that of fitting  $J^{(2)}$ 's, as can be seen by writing

$$I_{\gamma 1} - I_{\gamma 0} + 2(n-1) = \alpha\omega_n + \beta\omega_n^3 + \gamma\omega_n^5, \quad (5)$$

where  $n=1, 2, \dots$ , and  $I_{\gamma 1}$  is the spin of the lowest observed transition in the SD band. Subtracting the  $n$ th equation from the  $(n+1)$ th equation gives  $2 = \alpha\Delta\omega + \beta\Delta(\omega^3) + \gamma\Delta(\omega^5)$ . Approximating  $\Delta(\omega^p)$  by  $p\omega^{p-1} \times \Delta\omega$ , and dividing by  $\Delta\omega$ , gives Eq. (1), so the coefficients in Eqs. (2) and (5) are essentially the same (e.g.,  $\beta = B/3$ ). Possible discrepancies in spin caused by using differentials vs using finite differences were shown to be  $< 0.01$  for the cases of interest; the test data corroborated this.

Table I also lists the *AB* fits obtained with Eq. (5), under the headings *I* fit. *ABC* fits with Eq. (5), being four-parameter, with a  $4 \times 4$  error matrix, were also compared to *ABC* fits of Eq. (1). An analysis of some twenty fittings of SD bands, both artificial and from SD190, has been made. Of those cases satisfying  $|C| \lesssim 1000$ , the spins resulting from the two approaches differed by less than the spin uncertainties from the error matrices in all but one case; in that case the difference was just two standard deviations.

If one just wants a mathematical least-squares fit to

some preconceived span of the data, the spins and spin uncertainties from Eqs. (1) and (5) are rather comparable. However, the spin uncertainty from the error matrix in either approach is significantly smaller than the potential uncertainty, depending on the character of the data, arising from the vital question of the accuracy of using the same  $\{ABC\}$  in the fit-span region and the extrapolation region—a question common to both methods. To address this question, parts (a) of the figures show clearly and directly in the *data* the character and extent of any systematic departure of the fitted curve from the input data,  $4/\Delta E_\gamma$ . Furthermore, the points in these parts (a) show directly in the data the relative merits of an *AB* or an *ABC* fit (or the inadequacy of both), and provide information about the best span of fit. The parts (b) of the figures, which also contain the ingredients of the *I* fit method, contain derivative information that does not have this close connection with the data.

We conclude that the spins of SD bands in the mass  $\sim 190$  region, sufficiently intense to provide  $E_\gamma$  accuracy of 0.2 keV, can be determined to  $\pm 0.1$  (or better), more than adequate to permit the selection of a spin from candidates differing by  $1\hbar$ . Thus these spins can be used in such important considerations as pseudospin and pseudo-oscillator.<sup>7,8</sup>

This work was supported in part by the U.S. Department of Energy under Contracts No. DE-AC03-76SF-00098 (Lawrence Berkeley Laboratory) and No. W7405-ENG-48-(Lawrence Livermore National Laboratory).

\*Permanent address: University of California, Davis, CA 95616.

†Permanent address: Iowa State University, Ames, IA 5011.

‡Permanent address: Centre d'Etudes Nucléaires de Bordeaux-Gradignan, Institut National de Physique Nucléaire et de Physique des Particules, Le haut-vigneau 33170, Gradignan, France.

§Present address: University of Liverpool, Liverpool, L69 3BX, United Kingdom.

\*\*Present address: Rutgers University, New Brunswick, NJ 08903.

††Permanent address: University of Kentucky, Lexington, KY 40506.

<sup>1</sup>E. F. Moore *et al.*, Phys. Rev. Lett. **63**, 360 (1989).

<sup>2</sup>J. A. Becker *et al.*, Phys. Rev. C **41**, R9 (1990); D. Ye *et al.*, *ibid.* **41**, R13 (1990).

<sup>3</sup>C. W. Beausang *et al.*, Z. Phys. A **335**, 325 (1990).

<sup>4</sup>M. A. Riley *et al.*, Nucl. Phys. **A512**, 178 (1990).

<sup>5</sup>About a dozen other SD bands have been found in the mass  $\sim 190$  region, and most are in press or submitted.

<sup>6</sup>One method,  $J^{(2)}$  fitting, initiated and developed by one of us (J.E.D.) at University of California, Davis, was barely introduced in our first paper on superdeformed bands in the mass 190 region, Ref. 2, and is primarily discussed here. The other method preceeded the  $J^{(2)}$  approach, was initiated by one of us (N.R.) at Lawrence Livermore National Laboratory, and was developed and applied there [J. A. Becker *et al.*, in Proceeding of Conference on Nuclear Structure in the Nineties, Oak Ridge, TN, April, 1990, edited by N. R. Johnson (unpublished)].

<sup>7</sup>F. S. Stephens *et al.*, Phys. Rev. Lett. **64**, 2623 (1990).

<sup>8</sup>F. S. Stephens *et al.* Phys. Rev. Lett. **65**, 301 (1990).

<sup>9</sup>S. M. Harris, Phys. Rev. **138**, B509 (1965).

<sup>10</sup>M. A. Stoyer *et al.* (unpublished).